ELSEVIER

Journal of Non-Crystalline Solids 176 (1994) 189–199

JOURNAL OF NON-CRYSTALLINE SOLIDS

Sol–gel synthesis of SiO_2–P_2O_5 glasses

C. Fernández-Lorenzo [a,*], L. Esquivias [b], P. Barboux [c], J. Maquet [c], F. Taulelle [c]

[a] *Departamento Química Física and* [b] *Departamento Estructura y Propiedades de los Materiales, Universidad de Cádiz, Apdo.40, 11510 Puerto Real (Cádiz), Spain*

[c] *Chimie de la Matière Condensée, Université P. et M. Curie, 4 place Jussieu, 75005 Paris, France*

Received 16 August 1993; revised manuscript received 22 April 1994

Abstract

The synthesis of P_2O_5–SiO_2 glasses from solutions has been studied through gelation kinetics, Raman and nuclear magnetic resonance (NMR) spectroscopies. Different preparation methods are compared. The effect of the phosphorus precursor has been investigated. Phosphoric acid esters are not hydrolyzed and they do not yield condensation with silica. Reaction of anhydrous H_3PO_4 with Si–OR groups leads to the formation of Si–O–P bonds which are easily hydrolyzed. Only a few remain after addition of water and gelation. Therefore, P–Si homogeneity is difficult to achieve after gelation and the following drying and heat-treatment procedures. This absence of homogeneity is observed by solid-state magic angle spinning (MAS)-NMR and X-ray diffraction studies performed on gel samples heated at 300, 500 and 800°C in the case of xerogels and 500, 950 and 1140°C for aerogels.

1. Introduction

Phosphate-containing glasses have a potential interest in the field of optical fibers and coatings [1,2]. Such materials may be prepared with improved homogeneity through sol–gel gel processes [2]. However, when the starting precursors are trialkylphosphates ($OP(OR)_3$), up to 50% of the nominal phosphorus content may be lost during subsequent heat-treatments. The amount of loss depends on the preparation method [3] as well as on the precursor [4]. Better homogeneity obtained through improved methods such as ultrasonic mixing (sonogels [5]) allows larger amounts of phosphorus to be retained in the gels. However, the silicon–phosphorus homogeneity is still difficult to achieve without heat-treatment at temperatures greater than 800°C.

Silicon–oxygen bonds possess a large covalency associated with the stable fourfold coordination of silicon. Therefore, hydrolysis of these bonds through the usual nucleophilic substitution of alkoxy groups by hydroxyl groups is difficult. The rates of the hydrolysis and condensation reactions of silica can be increased when catalyzed through addition of acids or bases [6]. On the other hand, the P–O bond is covalent and, to our knowledge, the only well-known coordination of P is four. Nucleophilic substitution at the P site although possible is difficult and most of the hydrolysis observed in acidic medium may proceed from cleavage of C–O bonds [7]. Therefore, phosphate esters are only weakly reactive and do not usually yield condensation [8]. Raman spectroscopy has shown the existence of P–O–Si

* Corresponding author. Tel: +34-56 830 668. Telefax: +34-56 834 924.

SSDI 0022-3093(94)00410-0

bonds [9]. From our point of view, these bonds are only a small percentage of the various species. Tian et al. [10] have also reported the formation of silicon–phosphate bonds through cohydrolysis of phosphate esters and silicon alkoxide after a long reaction time. Recent ^{31}P nuclear magnetic resonance (NMR) spectra of phosphosilicate gels have demonstrated that only free orthophosphate species are found in the gels after hydrolysis and drying [4,11]. Moreover, Fernández-Lorenzo et al. [12] have observed through electron microscopy and energy-dispersive X-ray analysis measurements that the phosphate distribution is not homogeneous in the gels. Heterogeneities only vanish upon heat-treatment at temperatures higher than 950°C. The P–O–Si bonds only appear upon further heat-treatment at high temperature. From this point of view, phosphoric acid has been shown to be a more reactive precursor than phosphate triesters [4].

In the following, we describe the effect of different methods (simple gelation or ultrasonic mixing) and different phosphate precursors (esters or anhydrous phosphoric acid) dried with the aerogel method on the synthesis of phosphosilicate gels.

2. Experimental

After gelation, all gels were dried under hypercritical conditions following the process described by Zarzycki et al. [13]. Two types of gelation method were used, yielding two types of gels.

(1) The first type was made by conventional gelation in ethanol. These gels will be called aerogels in the following. However, some gels made for comparison were dried at 100°C in an oven and will be denoted xerogels. Equal volumes of tetraethoxysilane (TEOS) and ethanol containing the phosphate precursor were mixed. Hydrolysis and condensation were performed by addition of the appropriate amount of water. Two different phosphate precursors were used, triethylphosphate (TEP) and phosphoric acid (H_3PO_4). Solid anhydrous H_3PO_4 (Fluka) was used in order to study the role played by the phosphate with TEOS before hydrolysis was carried out.

(2) The second type, hereafter called sono-aerogel, was prepared by mixing the components under ultrasonic irradiation without using any common solvent. The method has been described elsewhere [3,5]. Activation of the reaction through ultrasonic dispersion increases the homogeneity at the molecular level and with this method there is less phosphate loss upon heat-treatment [5].

All liquid state NMR spectra were collected on a Fourier transform NMR spectrometer (Bruker AM 250) operating at the frequency of 101.256 MHz for ^{31}P (pulse width: 9 μs and recycling delay: 3 s) or 49.69 MHz for ^{29}Si (pulse width: 8 μs, recycling delay: 10 s; chromium acetylacetonate 1×10^{-2} M was added to increase the relaxation rate). Samples were placed in 8 mm NMR tubes, and then placed in 10 mm NMR tubes filled with C_6D_6 used as a deuterium lock-in of the magnetic field.

Solid-state NMR spectra were collected on a spectrometer (Bruker MSL400) equipped with magic angle spinning (MAS) Andrew type rotor rotated at a speed of approximately 8 kHz. They were measured at the frequency of 161.98 MHz for ^{31}P (pulse width: 2 μs recycling delay: 5 s) or 79.5 MHz for ^{29}Si (pulse width: 2 μs, recycling delay: 10 min for glasses and 2 min for aerogels up to 500°C).

Spectra are referenced to H_3PO_4 85% in water for ^{31}P and tetramethylsilane for ^{29}Si used as the 0 ppm references. As in the current convention, negative chemical shifts are in the high-field direction (more shielded atoms).

Raman spectra were recorded at 90° scattering geometry with a double monochromator (Jobin–Yvon U-1000), coupled to a photomultiplier (RCA 31034). The output pulses were analyzed with photon counting electronics. An Ar^+ laser with a power of 0.4 W at 514.5 nm was used as the exciting radiation source. The spectra here presented were treated with a smoothing method.

Chemical analysis were performed by atomic absorption at the CNRS Laboratory for chemical analysis in Vernaison (France).

3. Results

3.1. Gelation times

In the case of triethylphosphate, hydrochloric acid solutions in water (pH = 1.5) were used for the hydrolysis. The gelation times for a constant hydrol-

Table 1
Gelation times (in hours) for gels obtained from TEP with a constant hydrolysis ratio of 4 H_2O/Si and various P/Si

P/Si	TEP + TEOS	
	classic gel	sonogel
0.1	168	25
0.2	216	39
0.5	336	47
0.9	384	83

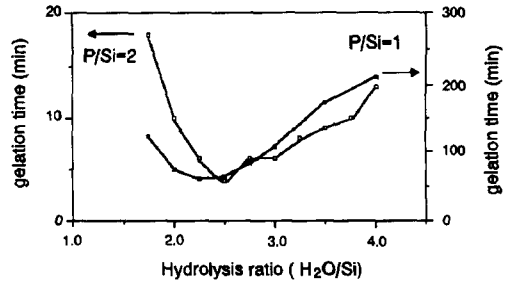

Fig. 1. Gelation time as a function of the P/Si ratio for a fixed hydrolysis ratio in the case of H_3PO_4/TEOS (□) and as a function of hydrolysis ratio for H_3PO_4/TEOS = 1 (■). Lines are drawn as a guide for the eye.

ysis ratio of 4 H_2O/Si and various P/Si are reported in Table 1. When H_3PO_4 was used as the phosphorus precursor, the variations of gelation times with the hydrolysis ratio H_2O/Si is reported in Fig. 1.

3.2. Chemical analysis

Chemical analyses were performed on gels immediately after drying and after heat-treatment under air at 950°C for 8 h. Results are reported in Table 2.

3.3. Liquid state ^{31}P NMR study

3.3.1. Case of TEP

Fig. 2 shows the ^{31}P NMR spectrum of TEP and TEOS, after hydrolysis and after aging for a few days leading to the gelation of a silica gel. This spectrum consist of a set of seven peaks centered around −1 ppm. This signal is characteristic of the phosphate triester where ^{31}P is magnetically coupled to the spins of the neighboring ^{1}H in the $OP(OCH_2CH_3)_3$ molecule, causing the $2 \times n \times \frac{1}{2} + 1$ couplings with $n = 6$.

3.3.2. Case of the H_3PO_4

In this case, an exothermic reaction is observed upon mixing TEOS and H_3PO_4. Typical ^{31}P NMR spectra obtained for different POH/Si ratio are reported in Fig. 3. The spectrum observed for POH/Si = 0.5 contains three different groups of signals located around +1.8 ppm (free H_3PO_4), −9.5 ppm ($-PO_4Q'^1$), −21 ppm (PO_4, Q'^2). Although not conventional, we denote by Q'^n a phosphate bound to n silicon atoms through P–O–Si bonds. The two last groups contain different peaks depending on the nature of the species bound to the central phosphate ion ($-Si(OR)_3$ or $-Si(OR)_2(OP-)$ and so on).

The percentage of each species is reported as a function of the P/Si ratio in Fig. 4(a) as well as the

Table 2
Results in molar ratios from chemical analysis performed on gels immediately after drying and after heat-treatment under air at 950°C for 8 h

Precursor	Procedure	H_2O/Si	P/Si nominal	P/Si dried	P/Si 950°C
H_3PO_4	xerogel	1	0.50	0.360	0.430
H_3PO_4	xerogel	2	0.50	0.340	0.340
H_3PO_4	xerogel	1	1.00	1.020	1.130
H_3PO_4	xerogel	4	2.00	2.000	0.700
H_3PO_4	aerogel	4	0.50	0.200	0.265
H_3PO_4	aerogel	4	1.00	0.410	0.470
TEP	aerogel	3	0.10	0.430	0.030
TEP	aerogel	3	0.85	0.210	0.310
TEP	sonoaerogel	3	0.10	0.042	0.026
TEP	sonoaerogel	3	0.85	0.430	0.230

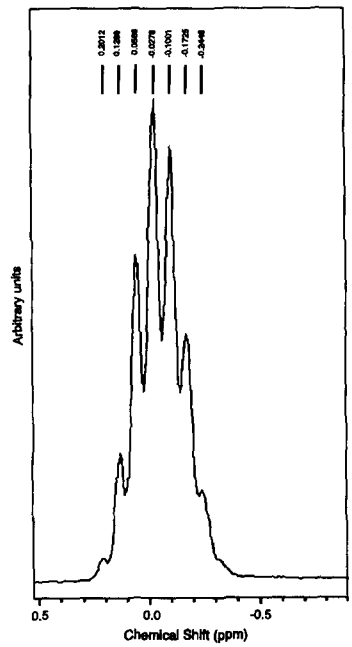

Fig. 2. ^{31}P liquid NMR spectrum of TEP/TEOS hydrolyzed and aged 1 week.

calculated number of Si–O–P bonds for each Si in Fig. 4(b).

The ^{29}Si NMR spectra for different P/Si ratios

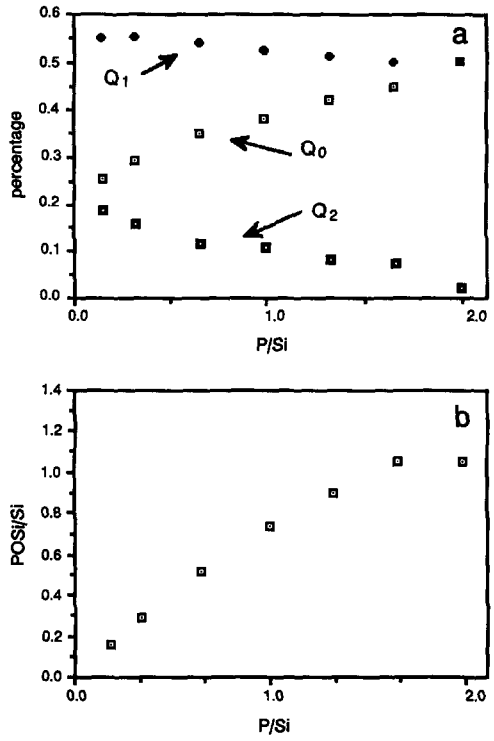

Fig. 4. (a) Percentage of the different phosphate species observed as a function of the P/Si ratio; (b) connectivity of Si derived from P/Si as a function of the P/Si ratio.

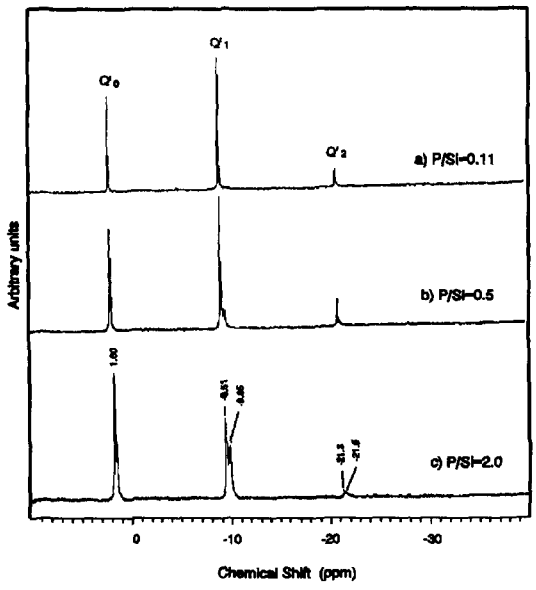

Fig. 3. Liquid-state ^{31}P NMR spectra of TEOS solutions with H_3PO_4 in ethanol for different P/Si ratios.

are reported in Fig. 5. We observe different signals corresponding to TEOS at -81.8 ppm, to Q'^1 (-91.2 ppm) and Q'^2 (-98 and -100.0 ppm) species. Here, we denote Q'^n the silicon connected to n P ions.

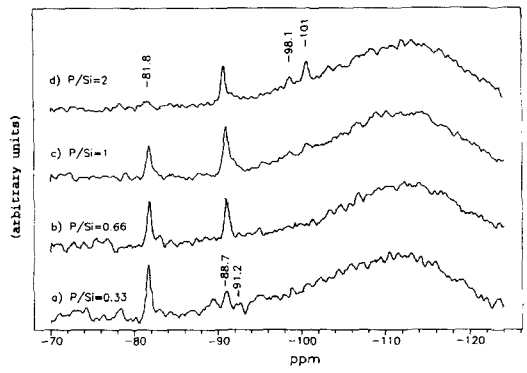

Fig. 5. Liquid state ^{29}Si spectra observed for different P/Si ratios.

3.3.3. Hydrolysis

Upon addition of water, components corresponding to PO_4 species bound to Si immediately disappear in the ^{31}P NMR spectra. The effect of water addition ($H_2O/Si = 0.5$) on a $P/Si = 0.5$ is shown in Fig. 6. Just after addition, only the peaks corresponding to phosphoric acid are observed (Fig. 6(b)). The peaks attributed to P–O–Si species (Fig. 6(a)) have disappeared.

3.4. Raman studies

TEP with its stoichiometric amount of water has been submitted to ultrasound to verify its non-reactivity as indicated by the ^{31}P NMR experiments. One month after beginning of the reaction, no evolution of the Raman bands is observed. This absence demonstrates that no hydrolysis of the TEP occurs in the conditions of our studies.

Therefore, the following study has been performed with anhydrous H_3PO_4 as the phosphorous precursor. The samples have been prepared according to the following sequence.

(A) Pure TEOS dissolved in EtOH, ratio 1:1. The Raman spectrum of this mixture is a superposition of individual spectra (ethanol and TEOS). No shift of the peak positions is observed (Fig. 7(a)).

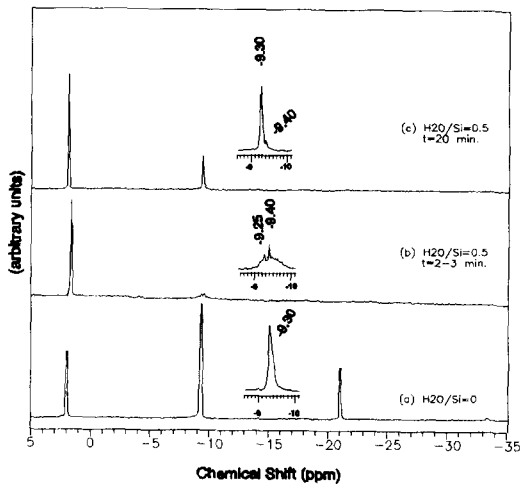

Fig. 6. ^{31}P NMR spectra of solutions $H_3PO_4/Si = 0.5$ (a) before addition of water; (b) two minutes after addition of 0.5 H20/Si; (c) 1 h later.

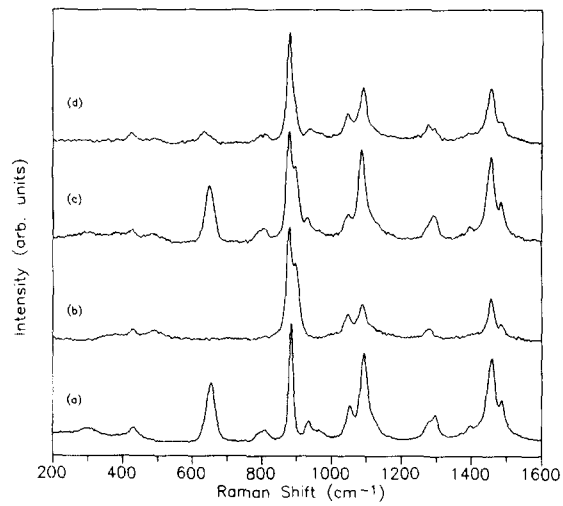

Fig. 7. Raman spectra of (a) solution A: TEOS in ethanol, (b) solution B: H_3PO_4 in ethanol; (c) theoretical addition of spectra (a) and (b); (d) solution C: mixture of A and B.

(B) Pure H_3PO_4 dissolved in EtOH. The spectrum of H_3PO_4 (Fig. 7(b)) is also the sum of the contributions of H_3PO_4 and ethanol. The peaks at 900, 497 and 384 cm^{-1} are characteristic vibration modes of the tetrahedral PO_4 molecule, the fourth mode is not observed because of overlapping. Other peaks correspond to the vibration modes of ethanol.

(C) H_3PO_4/TEOS/EtOH. When solutions described in paragraphs (A) and (B) are mixed, there is no superposition of the two spectra. In the Fig. 7(c) we observe the sum of both spectra in comparison with the experimental spectrum (Fig. 7(d)).

(D) H_3PO_4/TEOS/EtOH + H_2O. In Fig. 8 we show the effect of hydrolysis for a mixture in which the molar ratios are $P/Si = 1$ and $H_2O/Si = 1.5$.

3.5. Solid-state ^{31}P NMR studies

3.5.1. Case of TEP

Just after hypercritical drying, only two signals are observed in the ^{31}P NMR spectrum for the $P/Si = 0.1$ aerogel around 0 and -11.5 ppm (Fig. 9(a)). For higher temperatures of heat treatment, broad peaks appear at -25 and -37 ppm.

For larger ratios ($P/Si = 0.85$), a quite different behaviour is observed. Just after drying, the aerogel only contains Q^0 as demonstrated by the single NMR signal observed at 1 ppm (Fig. 10(a)). After

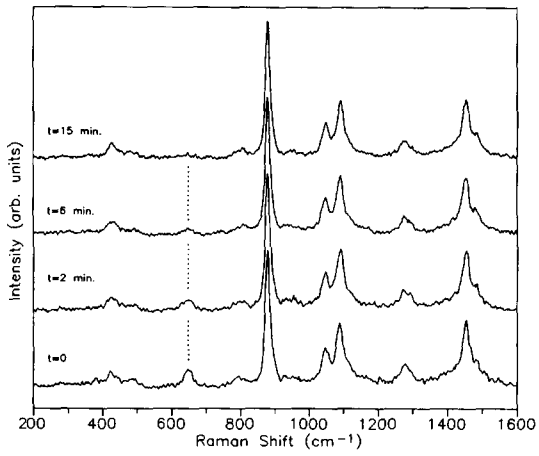

Fig. 8. Time evolution of the Raman spectrum of a solution of TEOS, H_3PO_4, EtOH and water in $P/Si = 1$, $H_2O/Si = 1.5$ ratios.

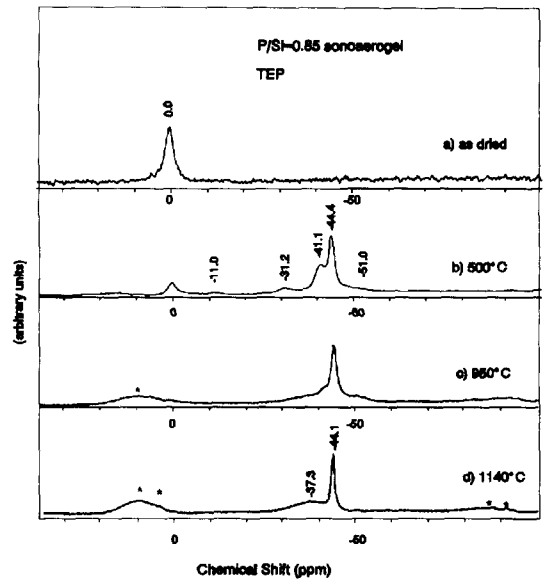

Fig. 10. ^{31}P MAS-NMR spectra of aerogels $TEP/Si = 0.85$: (a) after drying, (b) 300°C, (c) 950°C and (d) 1140°C. The asterisk indicates spinning-side bands.

the aerogel is heated above 500°C, weak signals appear at -10 and -30 ppm.

3.5.2. Case of phosphoric acid

^{31}P NMR spectra are reported in Fig. 11 for different temperatures of heat treatment. We observe different signals corresponding to free H_3PO_4, Q^1 species around -11 ppm, very weak peaks attributed to Q^2 (-25 ppm) and Q^3 (-31 ppm) and a group of peaks around -44 ppm which we again attribute to PO_4 in a Q^4 coordination.

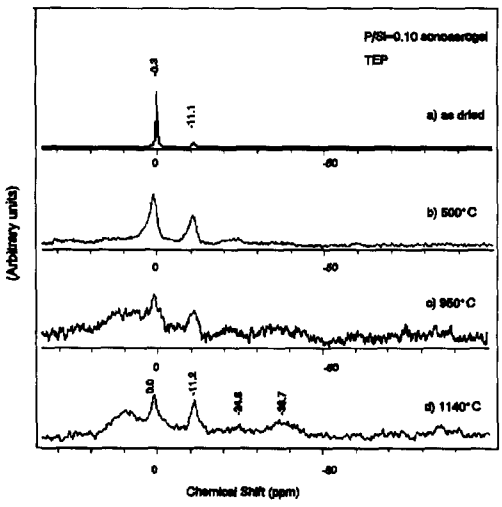

Fig. 9. ^{31}P MAS-NMR spectra of aerogels $TEP/Si = 0.1$: (a) after drying, (b) 500°C, (c) 950°C and (d) 1140°C.

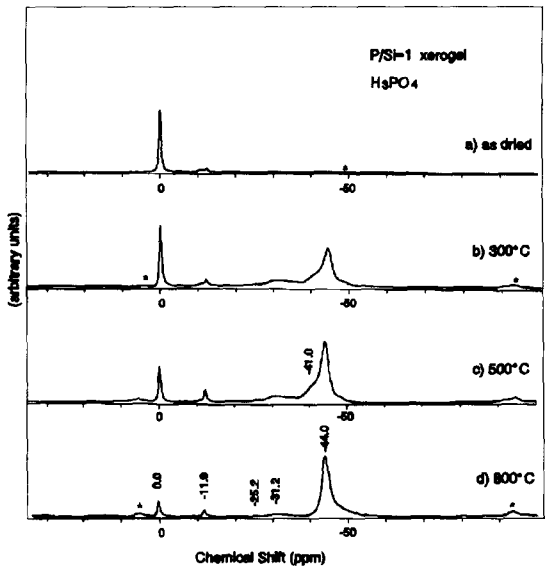

Fig. 11. ^{31}P MAS-NMR spectra of aerogels $H_3PO_4/Si = 1$: (a) after drying, (b) 300°C, (c) 500°C and (d) 800°C. The asterisk indicates spinning-side bands.

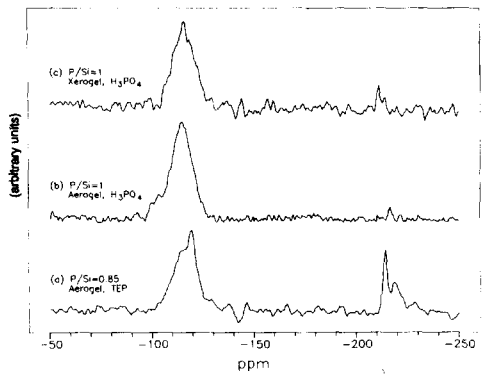

Fig. 12. ^{29}Si MAS-NMR spectra of aerogels H_3PO_4/Si = 0.5, xerogel H_3PO_4/Si = 0.5 and (c) aerogel TEP/Si = 0.5 after heat treatment at 950°C.

3.6. ^{29}Si MAS-NMR study

The ^{29}Si NMR spectra of these materials are qualitatively similar, independent of the starting precursor and the method used (Fig. 12).

4. Discussion

4.1. Gelation kinetics

4.1.1. Case of triethylphosphate

The gelation times are of the order of a few days and are of the same order as for pure silica gels. They were much shorter for sono-aerogels (hours) and this difference may be attributed to a more homogeneous mixing of the components. The gelation time increased with increasing P/Si ratio. If we assume, as shown later, that the phosphate species are inert, this increase may be explained by a dilution effect of TEOS or by an increase of viscosity due to the addition of TEP.

4.1.2. Gels from phosphoric acid

When H_3PO_4 was used as the phosphorus precursor, the gelation time decrease and was similar to the times observed with HF [6] or 4-dimethylaminopyridin (DMAP) [14] catalysis. For all P/Si ratios, we observed an onset of gelation at $H_2O/Si = 1.5$ (Fig. 1). Below this threshold no gel was obtained. Above, the gelation time decreased with amount of water added to a minimum then increased again for higher water contents. The hydrolysis ratio at which the minimum gelation time was observed increased with the amount of phosphoric acid added. The gelation time decreased with increasing phosphate content. Such results have been described in the case of acidic catalysis of gelation [15]. The gelation times are too short to be related only to acid catalysis and it will be argued in the following that the phosphate ions themselves play a significant role, similar to fluorides [6], in activating the cleavage of the Si–O–C bonds. However, phosphoric acid cannot be considered as a true catalyst since it must be present in a large amount to activate the condensation.

4.2. Chemical analysis

For all gels dried under hypercritical conditions, a large phosphorus loss (around 50%) was observed upon drying. Sono-aerogels retained larger amounts of phosphoric acid.

Xerogels made with H_3PO_4 and dried in an oven at 100°C, did not lose phosphorus upon drying at this temperature. Up to a ratio, P/Si = 1, no loss was observed upon heat-treatment, whereas, above this ratio, a loss was observed after heat-treatment at 950°C. Aerogels made from H_3PO_4 showed a loss of phosphorus upon drying although this loss was small compared with samples made out of TEP.

From this results, it is clear that none of the phosphate precursors used in this study allows a complete homogeneity of the gels that would minimize the phosphorus loss during hypercritical drying.

4.3. Study of the precursors solutions

4.3.1. Case of TEP

No change is observed in the ^{31}P NMR spectrum before and after mixing TEP and the TEOS, after hydrolysis, and after aging a few days leading to the gelation of a silica gel. Therefore, TEP does not interfere in the hydrolysis and condensation steps of TEOS. This lack of interference is in agreement with the large gelation times similar to those observed for pure TEOS.

4.3.2. Case of the H_3PO_4

In this case, our attribution is based on the analogy of these chemical shifts with similar signals

observed in polyphosphates [16]. This analogy also agrees with recent assignments of components in the spectra of silicophosphate glasses [4]. Similar chemical shifts would be observed if the phosphate was connected to other phosphate groups (the transformation of pyro- to polyphosphates). However, this connection is impossible because homonuclear condensation of polyphosphates never occurs spontaneously at room temperature in solutions. Moreover, the spin–spin coupling constants, $^2J_{P-P}$, would be observed in this case [16]. Therefore, we conclude that a set of reactions such as the following takes place:

$$-P(OH)_{3-n} + ROSi \rightarrow -P(OH)_{2-n}(OSi) + ROH \quad (1)$$

for $n = 0,1,2$.

When the POH/Si ratio increases, we observe a higher percentage of species at high chemical shift (around 0 ppm, Q'^0 species) in Fig. 4(a). From Fig. 4(b), we conclude that the connectivity of silicon progressively increases up to 1 Si–O–P bond for each silicon atom. This connectivity is the apparent limit in the liquid state. But, above the P/Si = 2 ratio, we observed that condensation becomes unlimited and solutions precipitate after a few hours without any hydrolysis.

In the peaks centered at −9 ppm, two peaks are observed. Therefore, both of these signals corresponding to Q'^1 phosphates are at −9.1 ppm to PO–Si(OR)$_3$ and at −9.5 ppm to PO–Si(OR)$_2$OP– or PO–Si(OR)–(PO)$_2$.

Our attribution is based on the fact that the intensity of the second peak relative to the first one increases with the P/Si ratio in agreement with the increasing probability of an Si connected to two P. Owing to the larger number of possible conformations and perhaps its more limited rotation, the second peak also appears broader. Similarly, at −20 ppm we observe signals which we attribute to PO_4 species of the Q'^2 type. These peaks are asymmetric and broader on the low chemical shift side. This feature is also explained by a larger variety of possible conformations of the Si atoms linked to these PO_4.

Our interpretation is confirmed by ^{29}Si NMR spectra reported in Fig. 5. We observe a signal that corresponds to the decrease of the signal attributed to TEOS (−81.8 pmm) and the increase of Q'^1 (−91.2 ppm) and Q'^2 (−98 and −100.0 ppm) species with increasing P/Si ratio. Here, we denote by Q'^n the silicon connected to n P ions. However, the peak intensities do not exactly correspond to the population expected from the ^{31}P NMR study. We think this behaviour can be attributed to relaxation effects.

4.3.3. Hydrolysis

The disappearance of the peaks attributed to P–O–Si species indicates a fast hydrolysis of the Si–O–P bonds following the reaction

$$H_2O + Si–O–P \rightarrow Si–OH + HO–P. \quad (2)$$

Since the reaction of phosphoric acid with SiOR groups is also very rapid, we assume that phosphoric acid acts as a catalyst of the hydrolysis reaction through the nucleophilic attack of Si instead of the usually invoked electrophilic protonation of the oxygen atoms of Si(OR)$_4$.

The two well known condensation reactions are [17]

$$SiOH + HOSi \rightarrow Si–O–Si + H_2O, \quad (3)$$

$$SiOH + ROSi \rightarrow Si–O–Si + ROH. \quad (4)$$

The water formed during reaction (3) should hydrolyze another SiOP bond very quickly but this procedure does not explain the fast gelation rate which depends on reaction (3) which is slow [18]. Therefore, we conclude that another reaction occurs, of the type

$$SiOH + SiOP \rightarrow Si–O–Si + POH. \quad (5)$$

This reaction has a faster rate than (3) and (4) and this rate explains the very fast gelation through an activation of the condensation of TEOS by H_3PO_4. For larger amounts of added water, all Si–O–P bonds will be rapidly hydrolyzed following reaction (2) and reaction (5) will not be possible. Writing the condensation rate through reaction (5) in the form of a second-order kinetics law (first-order in both reagents)

$$d[Si–O–Si]/dt = K_c[Si–OH][Si–O–P] \quad (6)$$

makes clear that if Si–O–P bonds have been hydrolyzed by reaction (2), the concentration [SiOP] is small and condensation will only occur through the slower pathway of reaction (3). This way probably

causes an increase of gelation time when too much water is added (Fig. 1, ■). Note that a similar effect has been reported in many other experiments on silica gelation [19].

After a short time and for small amounts of added water ($H_2O/Si = 0.5$, $POH/Si = 0.5$), we observe in the ^{31}P spectra that the intensity of Q^1 and Q^2 species increases again (Fig. 6(c)). This increase indicates that the small ratio of water used in this experiment has been consumed in the hydrolysis of Si–O–P bonds and the P–OH groups, regenerated through reaction (2), have reacted again with other Si–OR groups. Note that the signal corresponding to Q^1 P–O–Si species has changed. Before hydrolysis and just after, P are connected to SiO_4 monomers. After hydrolysis and condensation P ions are connected to highly branched SiO_4 units. Then, the nature of the Q^1 species is different before and after hydrolysis. This difference is indicated by slight changes both in chemical shifts and line widths. After hydrolysis, the Q^1 P ions are linked to condensed silicates and the slower motion produces wider lines.

As demonstrated by these-liquid-state NMR measurements, the Si–O–P bonds are easily hydrolyzed. Thus, we assume that H_3PO_4 acts as an hydrolysis and condensation catalyst, but it does not participate to the cross-linking of the structure. The resulting gel may be considered a silica gel with free H_3PO_4 trapped in the pores (Q^0 species) or adsorbed at the surface of the colloidal SiO_2 particles in the form of Q^1 species.

4.4. Raman studies

First, a decrease of the relative intensities of H_3PO_4 and TEOS characteristic vibrations is observed in Fig. 7(d). The peak at 654 cm^{-1}, attributed to Si–O–C vibrations, shifts towards a lower frequency (639 cm^{-1}). Its intensity also decreases and becomes comparable with the 807 cm^{-1} band. Mulder and Damian [20] observed a similar feature in their Raman study of the TEOS hydrolysis and polycondensation. The polarized 654 cm^{-1} band shifts to 600 cm^{-1} because of the TEOS dimer ($Si_2O(OC_2H_5)_6$), i.e., Si–O–Si bond formation. From this indication, we conclude that the shift towards 639 cm^{-1} is due to the formation of Si–O–P bonds. On the other hand, a comparison of TEOS/EtOH and H_3PO_4/TEOS/EtOH spectra indicates a decrese of intensity of the band at 1094 cm^{-1}, commonly attributed to Si–O–C vibrations. As a conclusion, there is a consumption of Si–O–C bonds and a decrease of the H_3PO_4 group symmetry related to the formation of Si–O–P bonds according to reaction (1), which explains the decrease of intensity of the Si–O–C and H_3PO_4 bands. However, this effect is rather limited on the H_3PO_4 peaks since the high ratio, $P/Si = 4$, used in this case, leaves a large amount of unreacted phosphoric acid as shown by the NMR study above.

In Fig. 8 we show the hydrolysis effect for a mixture in which the molar ratios are $P/Si = 1$ and $H_2O/Si = 1.5$. Two minutes after the addition of water, we observe a decrease of the 639 cm^{-1} band associated to Si–O–P vibrations. After 15 min this peak has almost disappeared. This fact is in agreement with reaction (2). We can also observe a decrease of the bands assigned to TEOS. The spectra becomes similar to a phosphoric acid/ethanol mixture (Fig. 7(b)) where the initial molar ratio H_3PO_4/EtOH would have been modified. This behaviour indicates a rapid hydrolysis and condensation of TEOS.

4.5. Solid-state ^{31}P NMR studies

4.5.1. Case of TEP

The NMR study of aerogels just after hypercritical drying indicates the poor reactivity of the phosphorus precursor. The only two signals observed in Fig. 9(a) can be attributed to Q'^0 (0 ppm) and Q'^1 (−11.5 ppm) species as already discussed in the previous part. For higher temperatures of heat-treatment, broad peaks appear at −25 and −37 ppm. We tentatively attribute these peaks to Q'^2 and Q'^3 species. The large number of Q^0 and Q^1 species remaining even after heat-treatment at 1140°C indicates that the average connectivity of PO_4 remains low. This low connectivity points out the lack of reactivity and a poor dispersion of phosphorus inside the material. The low signal-to-noise ratio is an indication of the small amount of phosphorus retained in the glass.

For larger ratios ($P/Si = 0.85$), just after drying, the aerogel only contains Q^0 as demonstrated by the

single NMR signal observed at 1 ppm (Fig. 10(a)). The peak remains sharp even without magic angle spinning. This fact indicates that this signal corresponds to quasi-liquid species with free rotation. In agreement with previous works [4,11], this result is expected in the absence of reaction between phosphate and silica up to this step of the process.

The weak signals at −10 and −30 ppm in Fig. 10(b), we again attribute to Q^1 and Q^3 species. The main difference with the case of smaller P/Si ratios is that, upon heating above 300°C, new signals are observed at −31, −41 and −44.4 ppm and weak peaks at −51 ppm. After heating above 950°C, the spectrum consists of only two signals. The first signal, at −37, is very broad and has large spinning side-bands whereas the second signal, at −44.4 ppm, has a small width with very weak spinning-side bands (see Fig. 10(c)). These chemical shifts correspond to condensed phosphate species. From a survey of the literature [21], the sharp peak observed at −44 ppm is attributed to the P ion in the $Si_5O(PO_4)_6$ crystalline phase [22] whereas the broad signal observed between −32 and −39 ppm is ascribed to P in a SiO_2–P_2O_5 glass [21] where it is found in the form of $OP–(OSi)_{3-x}(OP)_x$ $(0 < x < 3)$. On the other hand, we attribute the signal that appears between 300 and 950°C at +41 ppm due to traces of a crystalline $Si_2P_2O_7$ phase present in this temperature range of heat treatment.

4.5.2. Case of phosphoric acid

We assume that the small fraction of Q^2 and Q^3 species is due to the rapid hydrolysis in air of these groups (following reaction (2) above) which leads to the formation of H_3PO_4 observed even for species heated at temperatures > 300°C. Thus, we have attributed the peak at −10 ppm to PO_4 Q^1 species such as $(HO)_2OP–O–Si$ bonds at the surface of the silica network. We have assigned the broad set of signals around −44 ppm (peaks at −35, −41, −44 (sharp), −50 ppm) to different species of PO_4 connected to a set of $P_{4-n}Si_n$ second neighbours. Its intensity increases with the temperature of heat-treatment, indicating that the amount of P which has reacted with silica increases. These Q^4 species, which are still present in the spectra even after exposure to wet air, are more stable towards hydrolysis than the Q^2 and Q^3 species. As in the case of the TEP precursor, a large fraction of these species must be attributed to phosphate in the crystalline $Si_5O(PO_4)_6$ phase. The spectra of these produce the sharp signal at −44 ppm.

4.6. ^{29}Si MAS-NMR study

During the heat-treatment, we observe a behavior identical to those described by Szu et al. [4]. Therefore, we only briefly discuss the evolution of the spectra with temperature. After drying, all aerogels give a single broad peak at −112.2 ppm. These peaks are characteristic of Q'^4 Si species where the silicate tetrahedras are coordinated to four other silicon atoms. When the temperature of heat treatment increases, this peak shifts towards lower chemical shifts (from −112 to −116 ppm). This shift was observed by Dupree et al. [25] who attributed the shift to an increase in the number of Si–O–P bonds in the glass. Above 500°C, two sharp peaks appear around −213 and −219 ppm. These peaks are characteristic of the $Si_5(PO_4)_6$ crystalline phase and correspond to sixfold-coordinated silicons [23,24]. This crystalline phase also contains fourfold-coordinated silicon atoms whose NMR spectra have a componenent at −119 ppm [25,26]. This peak is resolved when there is a great amount of crystalline phase such as in the case of the TEP precursor (Fig. 12(c)).

From Fig. 12, we also observe the effect of the phosphorus precursor. From the intensity of the characteristic peaks of the crystalline phase (at −119, −213 and −219 ppm), we observe that the aerogel and xerogel samples made from H_3PO_4 (Figs. 12(a) and (b)) contain less crystalline phase than when the TEP precursor is used (Fig. 12(b)). However, they contain a larger amount of phosphate as shown in Table 2.

5. Conclusion

After a study of the precursor and mixing method, we conclude that the phosphorus losses increase when unreactive precursors are used.

In all cases (TEP or H_3PO_4 precursors) there is no Si–O–P chemical homogeneity resulting from gelation. In the case of TEP, bonds never appeared.

In the case of H_3PO_4, they appear in the first steps of the process, but they disappear on hydrolysis. However, the thermal reactions are different.

After heat treatment and exposure to air, there are larger amounts of phosphoric acid in the samples made from the phosphoric acid precursor whereas larger amounts of the crystalline $Si_5O(PO_4)_6$ phase are found when starting from TEP in samples heated above 800°C.

With the H_3PO_4 precursor, better homogeneity may be achieved with the minimum hydrolysis and protection from the air moisture before the final heat treatment, avoiding the cleavage of the P–O–Si bonds formed during the first steps of the process.

References

[1] S.G. Kosinski, D.M. Krol, T.M. Duncan, D.C. Douglass, J.B. MacChesney and J.R. Simpson, J. Non-Cryst. Solids 105 (1988) 45.

[2] D.C. Douglass, T.M. Duncan, K.L. Walker and R. Csencsits, J. Appl. Phys. 58 (1985) 197.

[3] L. Esquivias and J. Zarzycki, in: Ultrastructure Processing of Advanced Ceramics, ed. J.D. Mackenzie and D.R. Ulrich (Wiley, New York, 1987) p. 255.

[4] S.P. Szu, L.C. Klein and M. Greenblatt, J. Non-Cryst. Solids 143 (1992) 21.

[5] L. Esquivias, C. Fernandez-Lorenzo and J.M. Rodriguez-Izquierdo, Riv. Staz. Sper. Vetro 5 (1990) 85.

[6] M.W. Colby, A. Osaka and J.D. Mackenzie, J. Non-Cryst. Solids 82 (1986) 37.

[7] J.R. Cox and O.B. Ramsay, Chem. Rev. 64 (1964) 317.

[8] J. Livage, P. Barboux, M.T. Vandenborre, C. Schmutz and F. Taulelle, J. Non-Cryst. Solids 147&148 (1992) 18.

[9] R. Jabra, J. Phalippou, M. Prassas and J. Zarzycki, J. Chim. Phys. 78 (1981) 777.

[10] F. Tian, L. Pan, X. Wu and F. Wu, J. Non-Cryst. Solids 104 (1988) 129.

[11] S. Prabakar, K.J. Rao and C.N.R. Rao, J. Mater. Res. 6 (1991) 592.

[12] C. Fernandez-Lorenzo, J. Martin, L.M. Esquivias and E. Blanco, in: Chemical Processing of Advanced Materials, ed. L.L. Hench and J.K. West (Wiley, New York, 1992) ch. 20, p. 215.

[13] J. Zarzycki, M. Prassas and J. Phalippou, J. Mater. Sci. 17 (1982) 3371.

[14] R.P.J. Corriu, D. Leclercq, A. Vioux, M. Pauthe and J. Phalippou, in: Ultrastructure Processing of Advanced Ceramics, ed. J.D. Mackenzie and D.R. Ulrich (Wiley, New York, 1988) p. 113.

[15] M. Yamane, S. Inoue and A. Yasumori, J. Non-Cryst. Solids 63 (1984) 13.

[16] M.M. Crutchfield, C.F. Callis, R.R. Irani and G.C. Roth, Inorg. Chem. 1 (1962) 813.

[17] C.J. Brinker and G.W. Scherer, Sol–Gel Science (Academic Press, San Diego, 1990) ch. 3.

[18] J.C. Pouxviel and J.P. Boilot, J. Non-Cryst. Solids 94 (1987) 374.

[19] G. Orcel, PhD dissertation, University of Florida (1987).

[20] C.A. Mulder and A.A. Damian, J. Non-Cryst. Solids 93 (1987) 387.

[21] T.L. Weeding, B.H. de Jong, W.S. Veeman and B.G. Aitken, Nature 318 (1985) 352.

[22] A.E. Mal'shikov, Russ. J. Inorg. Chem. 32 (1987) 1383.

[23] T.L. Weeding, B.H. de Jong, W.S. Veeman and B.G. Aitken, Nature 318 (1985) 352.

[24] A.E. Mal'shikov, Russ. J. Inorg. Chem. 32 (1987) 1383.

[25] R. Dupree, D. Holland and M.G. Mortuza, Nature 328 (1987) 416.

[26] A.R. Grimmer, F. von Lampe and M. Mägi, Chem. Phys. Lett. 132 (1986) 549.